

# Numerical multiplexing and demultiplexing of digital holographic information for remote reconstruction in amplitude and phase

M. Paturzo,<sup>1,\*</sup> P. Memmolo,<sup>2</sup> L. Miccio,<sup>1</sup> A. Finizio,<sup>1</sup> P. Ferraro,<sup>1</sup> A. Tulino,<sup>2</sup> and B. Javidi<sup>3</sup>

<sup>1</sup>CNR-Istituto Nazionale di Ottica Applicata & Istituto di Cibernetica, via Campi Flegrei 34, 80078-Pozzuoli (NA), Italy

<sup>2</sup>DIET, Università di Napoli "Federico II", Via Claudio 21, 80125 Napoli, Italy

<sup>3</sup>ECE Department, University of Connecticut, U-157, Storrs, Connecticut 06269, USA

\*Corresponding author: melania.paturzo@inoa.it

Received June 20, 2008; revised September 11, 2008; accepted September 13, 2008; posted October 9, 2008 (Doc. ID 97736); published November 12, 2008

We investigate the possibility to multiplexing (Mux) and demultiplexing (de-Mux) numerically digital holograms (DHs) with the aim of optimizing their storage and/or transmission process. The DHs are multiplexed and demultiplexed thanks to the unique property of the digital holography to numerically manage the complex wavefields. We show that it is possible to retrieve correctly quantitative information about the amplitude and phase of one hundred DHs. This result can be useful to transmit efficiently, in terms of reduced amount of data, the DHs from the recording head to a remote display unit. © 2008 Optical Society of America  
OCIS codes: 090.1995, 100.2000, 180.0180, 100.0100, 070.0070, 070.2615.

Multiplexing digital holograms (DHs) means encoding two or more holograms in a single one by optical or numerical techniques. Multiplexing (Mux) recording of DHs has been proved for the measurement of some object properties, as the state of polarization, dynamical phenomena, or three-dimensional (3D) mechanical deformations by a single image acquisition [1,2]. Other applications of Mux techniques in holography regard the investigation of ultrafast events [3]. A pulsed digital microholographic system with spatial angular Mux for recording ultrafast processes of the femtosecond order is demonstrated with the aim to study the dynamics of the laser-induced ionization of air [4]. Mux has also found useful applications in multiwavelength DHs in order to address the issue of 3D imaging in full colors or to desensitize the interferometric gauge by an higher synthetic wavelength [5,6].

In all the mentioned approaches, spatial Mux of DHs is obtained by recording simultaneously more than one fringe pattern on the same CCD. All the holograms are superimposed in one composite CCD frame, and each of them can be independently reconstructed through a digital spatial filtering if the image bandwidth of each hologram is sufficiently low. Demultiplexing (de-Mux) is obtained as follows. Each individual hologram is filtered out by performing the digital Fourier transform (FT) of the multiplexed hologram. The filtering in Fourier spectral domain is done by selecting a passband corresponding to the desired hologram. Then the inverse FT on the filtered result is computed with the aim of obtaining a separate DH for each of the multiplexed signals. The size of the object spectrum in the Fourier plane determines how many DHs can be efficiently multiplexed. Up to three DHs have been multiplexed without decreasing the spatial resolution, that is, using all the aperture of the CCD array [1,3–5].

Nonetheless, it is simple to understand that the bandwidth of each single hologram depends on the optical configuration adopted for its recording. Two common types of holograms exist: image-plane holograms and Fresnel holograms. With image-plane holograms an objective lens is used to precondition the object wave, whereas with Fresnel holography the object field propagates in free space until it reaches the sensor. The space-bandwidth product (SBP) for image-plane holograms is inversely proportional to the focal length of the lens and proportional to the object magnification [7]. Therefore, if we use lenses with short focal length to obtain large magnification, the hologram SBP is such that no more than two holograms can be separated in the Fourier plane and, therefore, optically multiplexed.

To overcome this problem, we propose a novel approach to numerically Mux/de-Mux DHs recorded in the microscopic configuration. Exploiting the unique capability of a DH to numerically manage the complex wavefronts, we reconstruct the object wave field at an intermediate plane, that is, the back focal plane (BFP) of the imaging lens. In this plane the complex-value array, corresponding to the object wavefield, is proportional to the FT of the wave complex amplitude at an input plane. Therefore, we obtain only the spectrum of the object wave field, removing the contribution of the carrier frequencies (that is, the chirped-phase factor coming from the interference between the plane reference beam and the curvature of the object beam introduced by the microscope objective). Then, the complex-value arrays are stitched in order to encode up to 100 DHs in a single computer-generated hologram ( $512 \times 512$  complex-value matrix). This kind of complex hologram is useful also in the de-Mux procedure. In fact, it is easier to separate the spectra of multiplexed holograms in

respect to the standard method, that is, performing the digital FT of the hologram.

This technique can be thought of as two-dimensional (2D) frequency-division Mux (FDM) [8]. FDM is a widely used form of signal Mux where multiple baseband signals are modulated on different-frequency carrier waves and added together to create a composite signal. Our method can be considered the spatial analog of the FDM technique. In fact, a spectral shift, that is a spatial carrier frequency, is applied to each object spectrum. Then all the spectra are added together to create a composite complex hologram. This technique could be useful to optimize the transmission of DHs from the recording head and the display unit being in separate locations (i.e., experiments performed in such environments as the International Space Station or submarines [9,10]). Some efforts have been already made to provide algorithms to efficiently compress holograms for digital storage and transmission of 2D and 3D images [11,12].

First, we will show how the holograms are multiplexed and then how the multiplexed hologram is processed in order to reconstruct all 100 amplitude and phase maps. Finally, these reconstructed images will be compared with those obtained by the original holograms, and the distortions caused by the Mux are evaluated.

The 100 holograms are acquired by means of a Mach-Zehnder interferometric microscope, superposition unit of which is shown in Fig. 1. The laser wavelength is 532 nm, and the microscope objective (MO) has a focal length  $f=9.0$  mm. The CCD detector has  $1280 \times 1024$  square pixel, the size of which is  $P_{\text{CCD}}=6.7 \mu\text{m}$ . The specimen is an *in vitro* mouse preadipocyte 3T3-F442A cell. It has been monitored for 25 h to investigate its activities, and 100 holograms have been recorded with an acquisition rate of four frames/hour. Moreover, a reference hologram is acquired in a area of the sample far from the cell in order to calculate the phase retardation caused only by the cell subtracting the phase shift due to the culture medium.

The holograms are reconstructed through a Fresnel-Kirchoff integral [13]. To multiplex the holograms, each is reconstructed in the BFP of the MO. In fact, the complex wave field in the BFP is proportional to the FT  $F(\dots)$  of the complex amplitude of the wave at an input plane, regardless of its distance  $d_0$  from the lens according to the equation [14]

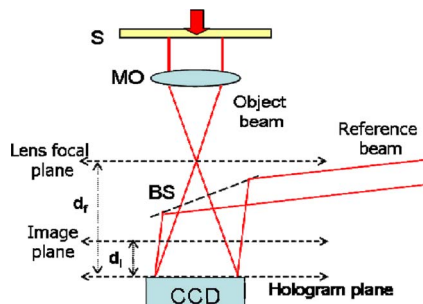


Fig. 1. (Color online) Superposition unit of the DH setup: S, sample; BS, beam splitter; MO, microscope objectives.

$$g(x,y) = h_l h_d F\left(\frac{x}{\lambda f}, \frac{y}{\lambda f}\right), \quad (1)$$

where  $h_d = \exp[i\pi(x^2 + y^2)(d_0 - f)/\lambda f^2]$  is a phase factor depending on  $d_0$  while  $h_l = (i/\lambda f)\exp(-i4\pi f/\lambda)$ .

In Fig. 2a the amplitude reconstruction of one hologram in the BFP, at the distance  $d_f=400$  mm from the hologram plane, is shown. The value of the pixel of reconstruction  $PR_f = \lambda d_f / (NP_{\text{CCD}})$ , that is, the pixel size in the reconstruction plane, is  $62 \mu\text{m}$  and corresponds to  $\Delta f = d_f / f NP_{\text{CCD}} = 13 \text{ mm}^{-1}$  in the spatial frequency domain, where  $N$  is the number of CCD pixels [13]. The inset in Fig. 2a shows the FT amplitude of the same hologram. It is clear that only few holograms could be multiplexed in the Fourier plane, because of size of the hologram FT. Then, we choose a mask to filter each hologram in the BFP. The small frame in Fig. 2a indicates the shape and the dimension of the used filtering window,  $50 \times 50$  pixels around the carrier frequency of the object spectrum, whose position depends on such geometrical parameters as the angle between the reference and the object beams and on the reconstruction distance  $d$ . The transmittance of the mask is 1 within the frame and 0 outside.

Obviously, reducing the dimension of the filtering window will increase the number of holograms we can encode in a single hologram. On the other hand, the size of the filtering window should be larger than the object bandwidth in order to retain the spectral information. However, for a fixed object, the choice of a correct filtering window depends also on  $d_f$  and  $f$ , since the value of  $\Delta f$  depends on their ratio. To properly multiplex the holograms in the BFP, we join together the filtered spectra shifting the carrier frequency of each hologram  $h_{m,n}$  by a value  $\vec{s} = (m\vec{x} + n\vec{y})p$  where  $m$  and  $n$  are integers ranging from 1 to 10 and  $p$  is the size of the filtering window. The amplitude of the synthetic spectrum obtained in this way is shown in Fig. 2b. The hologram  $h_{1,1}$  corresponds to the reference hologram. This complex-value array contains the information about the phase and the amplitude of all 100 holograms; it has to be transmitted with the Mux key. In fact, the numerical de-Mux needs the precise knowledge of the frequencies of the spatial carrier waves of all the holograms. Therefore, the receiver can demultiplex the synthetic

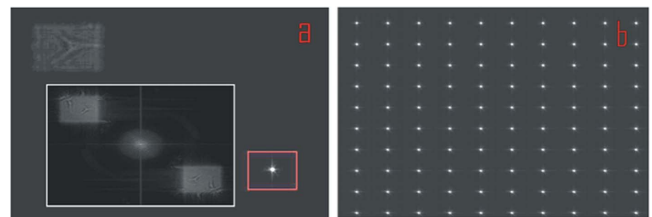


Fig. 2. (Color online) a, Amplitude reconstruction of one hologram in the BFP. The small frame indicates the used filtering window,  $50 \times 50$  square pixels around the carrier frequency of the object spectrum. The inset shows the amplitude of the hologram FT. b, Amplitude of the synthetic spectrum obtained by the numerical Mux in the BFP of 100 DHs.

spectrum and reconstruct all holograms only knowing the Mux key. In the de-Mux process the hologram composed in the BFP is filtered by selecting one by one the single holograms that, then, are numerically reconstructed in the image plane by means of a two-step reconstruction algorithm. In the first step the wave field is reconstructed in the hologram plane, setting the reconstruction distance  $d = -d_f$ , and then the in-focus amplitude and phase reconstruction in the image plane are obtained setting  $d = d_i$  where  $d_i$  is the distance between the hologram and the image plane (Fig. 1).

We adopt the double-step reconstruction algorithm to make the pixel of reconstruction in the image plane independent from the distance  $d_f$  and equal to  $PR_i = \lambda d_i / NP_{\text{CCD}}$ , like in a standard Fresnel reconstruction process [15]. Therefore we can compare the reconstructions obtained by the proposed FDM technique to those one coming from the original holograms.

In Fig. 3 the amplitude and phase reconstructions of one hologram as acquired by the CCD (left) and after the Mux/de-Mux process (right) are shown. Comparing the two kind of reconstructions, the distortion caused by the filtering process is not evident. In Fig. 4 we have plotted the difference between the two phase reconstructions in order to evaluate the distortion. Then we calculated the mean value and the variance of the 2D distribution of this phase difference. The mean value is 0.068 rad with a variance of  $1 \times 10^{-3}$  rad, while the maximum value is 0.23 rad. Looking at Fig. 4, it is clear that the maximum phase difference is on the cell border. This result is caused by the use of the filtering window that acts as a band-pass filter with limited bandwidth, cutting the high spatial frequencies owing to the edges.

In conclusion, we proposed an all-numerical Mux/deMux technique for DHs recorded in the microscope configuration. We demonstrated that up to 100 DHs can be multiplexed and demultiplexed correctly using this method. The phase distortions caused by this procedure have been evaluated and are on average

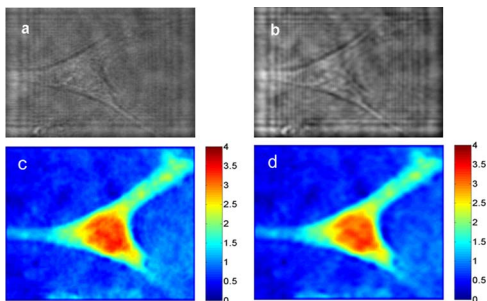


Fig. 3. (Color online) (a, c) Amplitude and phase reconstructions of one hologram as acquired by the CCD (Media 1) and (b, d) after the Mux/de-Mux process (Media 2).

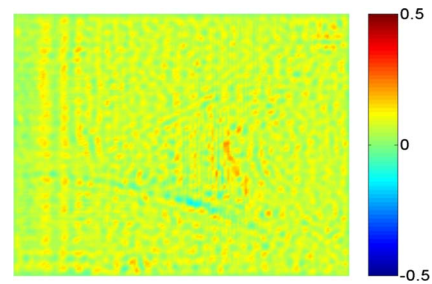


Fig. 4. (Color online) Single-frame excerpts from the movie of the 2D distribution of the difference between the two phase reconstructions in Figs. 3c and 3d (Media 3).

less than 0.07 rad. This technique could be useful to perform an efficient storage and/or fast transmission of DHs from the recording head to the display unit.

This research is funded from the European Community's Seventh Framework Programme FP7/2007-2013 under grant agreement 216105 "Real 3D."

## References

1. T. Colomb, F. Dürr, E. Cuche, P. Marquet, H. G. Limberger, R.-P. Salathé, and C. Depeursinge, *Appl. Opt.* **44**, 4461 (2005).
2. P. Picart, E. Moisson, and D. Mounier, *Appl. Opt.* **42**, 1947 (2003).
3. Z. Liu, M. Centurion, G. Panotopoulos, J. Hong, and D. Psaltis, *Opt. Lett.* **27**, 22 (2002).
4. X. Wang, H. Zhai, and G. Mu, *Opt. Lett.* **31**, 1636 (2006).
5. J. Kühn, T. Colomb, F. Montfort, F. Charrière, Y. Emery, E. Cuche, P. Marquet, and C. Depeursinge, *Opt. Express* **15**, 7231 (2007).
6. C. J. Mann, P. R. Bingham, V. C. Paquit, and K. W. Tobin, *Opt. Express* **16**, 9753 (2008).
7. A. Stern and B. Javidi, *J. Opt. Soc. Am. A* **25**, 736 (2008).
8. H. P. E. Stern, and S. A. Mahmoud, *Communication Systems: Analysis and Design* (Prentice Hall, 2003).
9. I. Zegers, L. Carotenuto, and C. Evrard, *Microgravity Sci. Technol.* **18**, 165 (2006).
10. J. Watson, S. Alexander, and G. Craig, *Meas. Sci. Technol.* **12**, L9 (2001).
11. K. Khare and N. George, *Opt. Lett.* **28**, 1004 (2003).
12. T. J. Naughton, J. B. McDonald, and B. Javidi, *Appl. Opt.* **42**, 4758 (2003).
13. U. Schnars and W. P. O. Jüptner, *Meas. Sci. Technol.* **13** R85 (2002).
14. B. E. A. Saleh, and M. C. Teich, *Fundamentals of Photonics* (Wiley-Interscience, 1991).
15. F. Zhang, I. Yamaguchi, and L. P. Yaroslavsky, *Opt. Lett.* **29**, 1668 (2004).